Interaction of (4-Hydroxyphenyl)pyruvate Dioxygenase with the Specific Inhibitor 2-[2-Nitro-4-(trifluoromethyl)benzoyl]-1,3-cyclohexanedione†

Michael Kavana and Graham R. Moran*

Department of Chemistry and Biochemistry, University of Wisconsin−Milwaukee, 3210 North Cramer Street, Milwaukee, Wisconsin 53211-3029

Received April 25, 2003; Revised Manuscript Received July 1, 2003

ABSTRACT: (4-Hydroxyphenyl)pyruvate dioxygenase (HPPD) is a non-heme Fe(II) enzyme that catalyzes the conversion of (4-hydroxyphenyl)pyruvate (HPP) to homogentisate as part of the tyrosine catabolism pathway. Inhibition of HPPD by the triketone 2-[2-nitro-4-(trifluoromethyl)benzoyl]-1,3-cyclohexanedione (NTBC) is used to treat type I tyrosinemia, a rare but fatal defect in tyrosine catabolism. Although triketones have been used for many years as HPPD inhibitors for both medical and herbicidal purposes, the mechanism of inhibition is not well understood. The following work provides mechanistic insight into NTBC binding. The tautomeric population of NTBC in aqueous solution is dominated by a single enol as determined by NMR spectroscopy. NTBC preferentially binds to the complex of HPPD and FeII [HPPD·Fe(II)] as evidenced by a visible absorbance feature centered at 450 nm. The binding of NTBC to HPPD·Fe(II) was observed using a rapid mixing method and was shown to occur in two phases and comprise three steps. A hyperbolic dependence of the first observable process with NTBC concentration indicates a pre-equilibrium binding step followed by a limiting rate ($K_1 = 1.25 \pm 0.08$ mM, $k_2 = 8.2 \pm 0.2$ s^{-1}), while the second phase ($k_3 = 0.76 \pm 0.02$ s^{-1}) had no dependence on NTBC concentration. Neither K_1, k_2, nor k_3 was influenced by pH in the range of 6.0−8.0. Isotope effects on both k_2 and k_3 were observed when D_2O is used as the solvent (for k_2, $k_h/k_d = 1.3$; for k_3, $k_h/k_d = 3.2$). It is therefore proposed that the bidentate association of NTBC with the active site metal ion (k_2) precedes the Lewis acid-assisted conversion of the bound enol to the enolate (k_3). Although the native enzyme without substrate reacts with molecular oxygen to form the oxidized holoenzyme, the HPPD·Fe(II)·NTBC complex does not. When the complex is exposed to atmospheric oxygen, the absorbance feature associated with NTBC binding does not diminish over the course of 2 days. This means not only that the HPPD·Fe(II)·NTBC complex does not oxidize but also that the dissociation rate constant for NTBC is essentially zero because any HPPD·Fe(II) that formed would readily oxidize in the presence of dioxygen. Consistent with this observation, EPR spectroscopy has shown that only 2% of the HPPD·Fe(II)·NTBC complex forms an NO complex as compared to the holoenzyme.

Naturally occurring diketone and triketone alkaloids are produced by a number of myrtaceous plants (*1*) and lichens (*2*). These compounds are employed as allelopathic agents, synthesized to prevent the growth of surrounding plants and/or microbes (*3*). The mode of action of this family of inhibitors is the specific inhibition of (4-hydroxyphenyl)-pyruvate dioxygenase (HPPD)[1] (*4*−*6*). HPPD, an α-keto acid-dependent non-heme iron(II) dioxygenase, catalyzes the second step in the catabolism of tyrosine (Scheme 1), the conversion of (4-hydroxyphenyl)pyruvate (HPP) to homogentisate. By inhibiting the production of homogentisate, tocopherols and plastoquinones can no longer be synthesized (*7*). This inhibition results in decreased levels of chlorophyll and carotenoid production, as evidenced by bleaching of the affected plants. Since the initial discovery of these molecules, intensive synthetic efforts have seen the development of many such molecules that specifically inhibit HPPD for use as herbicides (*8*−*12*). Several of these inhibitors, including mesotrione, sulcotrione, and isofluxatole, are currently in use as selective broad leaf herbicides (*13*−*15*).

In humans, defects in the tyrosine catabolism pathway range from the relatively mild symptoms of type II tyrosinemia (*16*, *17*) to the fatal, if untreated, type I tyrosinemia (*18*, *19*) (Scheme 1). Type I tyrosinemia is the most serious defect in the pathway, arising from a dearth of active fumarylacetoacetase, the enzyme that catalyzes the cleavage of fumarylacetoacetate to acetoacetate and fumarate (*20*). In the absence of active fumarylacetoacetase, fumarylacetoacetate accumulates in the liver and is either saturated or decarboxylated to succinylacetoacetone or succinylacetone, respectively. The accumulation of these highly electrophilic molecules causes the early onset of liver cirrhosis and primary liver cancer as well as inhibition of heme synthesis at porphobiligen synthase, resulting in severe anemia.

† This research was supported by the National Institutes of Health (Grant DK59551) to G.R.M. and in part by an American Chemical Society, Petroleum Research Fund Grant to G.R.M. (Grant 36169-G4).

* To whom correspondence should be addressed. Phone: (414) 229-5031. Fax: (414) 229-5530. E-mail: moran@uwm.edu.

[1] Abbreviations: NTBC, 2-[2-nitro-4-(trifluoromethyl)benzoyl]-1,3-cyclohexanedione; HEPES, *N*-(2-hydroxyethyl)piperazine-*N*′-2-ethanesulfonic acid; HPPD, (4-hydroxyphenyl)pyruvate dioxygenase; HPP, (4-hydroxyphenyl)pyruvate; EPR, electron paramagnetic resonance spectroscopy; HMBC, heteronuclear multibond correlation; HSQC, heteronuclear single-quantum coherence; DEPT, distortionless enhancement by polarization transfer.

10.1021/bi034658b CCC: $25.00
Published on Web 08/08/2003

Scheme 1

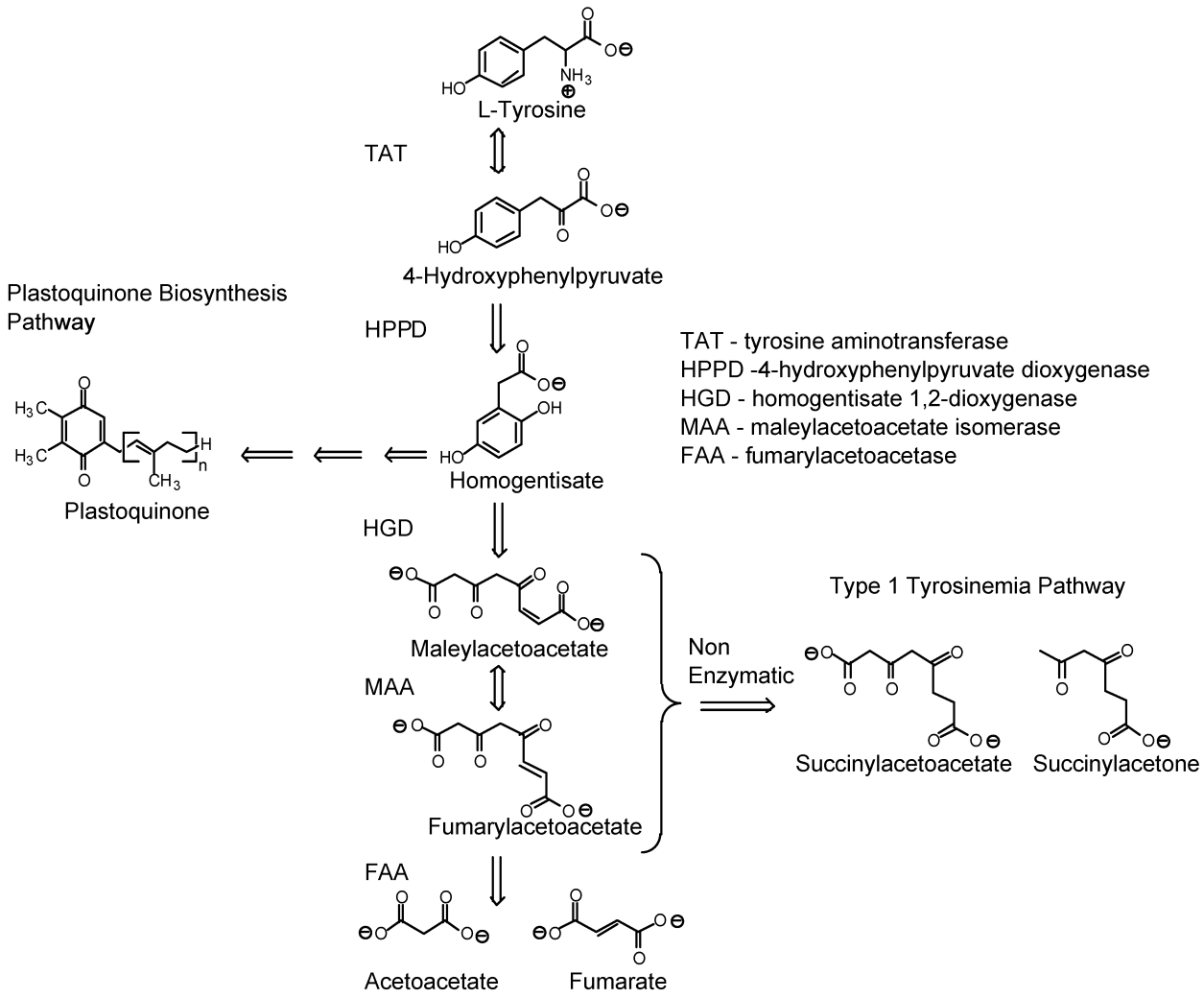

Although 2-[2-nitro-4-(trifluoromethyl)benzoyl]-1,3-cyclohexanedione (NTBC) was one of the first triketones that was developed as an herbicide (*21*), the dramatic effect of this molecule on a number of type I tyrosinemia sufferers in 1991 combined with the lethality of the disease led to its use as a therapeutic agent in the absence of the usual phase II and III clinical trials (*22*). In treated patients, the levels of excretion of succinylacetoacetone and succinylacetone diminished to the detection limit and the induced anemia was alleviated. Elevated blood tyrosine levels caused by the accumulation of HPP and the reversibility of the first enzyme in the catabolism pathway, tyrosine aminotransferase, resulted in ocular lesions that are a side effect of NTBC treatment when a tyrosine-deficient diet is not maintained (*23*). The adoption of NTBC as a theraputic agent for type I tyrosenemia has been very successful, and patients can now live normal lives without the need for liver transplants (*24*).

Despite the success of NTBC as a medical treatment, many of the fundamental details of NTBC activity have not been definitively established for HPPD from any source. The dominant tautomeric state of the inhibitor in aqueous solution has not been rigorously determined. Although it has been both suggested that NTBC interacts with the ferric form of the enzyme (*25*) and determined that the diketone of isoxaflutole binds to the ferrous form (*8*), it has not been definitively shown whether NTBC binds to the Fe(II) or Fe(III) form of HPPD to bring about inhibition. Moreover, detailed binding kinetic studies have not been undertaken to establish the mechanism of association, nor has the dissociation constant for the complex of HPPD and NTBC been rigorously measured. In this report, we will address these fundamental biochemical aspects of NTBC inhibition.

EXPERIMENTAL PROCEDURES

Materials. HPPD from *Streptomyces avermitilis* was purified as previously described (*26*). NTBC was provided as a gift from Swedish Orphan AB. HPP, HEPES, deuterium oxide (100%), potassium phosphate, ferric ammonium sulfate, and ferrous sulfate were purchased from ACROS. Dithiothreitol was purchased from Sigma. EPR tubes (707 J. Young) were from Wilmad.

NMR Spectroscopy. All NMR studies were performed at 278 K with a 6 mM solution of NTBC in 20 mM phosphate buffer at pH 7.0 with sufficient D_2O to obtain lock. The water signal was used as an internal reference and set to 5.018 ppm. Spectra were acquired on a Bruker DRX500 spectrometer operating at 500.13, 125.77, and 470.56 MHz for ^{1}H, ^{13}C, and ^{19}F, respectively. Proton and ^{19}F detection experiments were performed using a broadband inverse probe (BBI) with triple axis gradients, while for ^{13}C detection, a broad-

band observe (BBO) probe was utilized. In all experiments, standard pulse sequences from the Bruker library were employed. For one-dimensional ^{1}H spectra, water suppression was applied using the WATERGATE pulse sequence (*27*). Two-dimensional ^{1}H{^{13}C}HSQC and HMBC experiments were carried out using the gradient-selected versions of the experiment. For all ^{19}F NMR experiments, the proton channel of the probe was tuned to ^{19}F. ^{19}F{^{13}C} HMQC and HMBC experiments were thus performed without ^{1}H decoupling and optimized for coupling constants of 270 and 7 Hz, respectively.

Observation of Steady-State Inhibition. Enzyme assays were carried out using a model DW1 Hansetech Oxygraph oxygen electrode. The 2 mL reaction mixture contained 1 mM dithiothreitol, 250 nM HPPD, 20 μM ferrous sulfate, and atmospheric oxygen ($\sim$250 μM) in 20 mM HEPES buffer (pH 7.0). After the background rate of oxygen consumption due to Fenton chemistry was established, the reaction was initiated with the addition of 150 μM HPP and inhibited with 25 μM NTBC. NTBC concentrations were determined using the extinction coefficient determined by weight ($\epsilon_{257} = 20\,500\ M^{-1}\ cm^{-1}$).

UV−Visible Spectra of NTBC Bound to HPPD. NTBC binding to the HPPD·Fe(II) complex was observed on a Hi-Tech model SF61-DX2 stopped-flow spectrophotometer. A 4 mL solution of 220 μM apo-HPPD in 20 mM HEPES buffer (pH 7.0) was made anaerobic in a tonometer at 4 °C by 54 alternating exchanges of vacuum and argon with time for equilibration between each set of three cycles. Once the solution was anaerobic, ferrous sulfate was added from a sidearm to achieve a final concentration of 200 μM. The tonometer was mounted onto the stopped-flow instrument, and the spectrum (from 300 to 700 nm) of the holoenzyme (100 μM) was recorded by mixing with an anaerobic buffer. A solution containing 1.63 mM NTBC in 20 mM HEPES (pH 7.0) was made anaerobic by sparging with argon for 10 min prior to the solution being mounted on the stopped-flow instrument. The NTBC solution was mixed with holo-HPPD, and the spectrum was recorded. The resulting spectrum was then corrected by subtracting the NTBC and holo-HPPD spectral contributions to give the HPPD·Fe(II)·NTBC binding feature.

Stopped-Flow Kinetic Measurements. The rate of formation of the HPPD·Fe(II)·NTBC complex was measured using a stopped-flow spectrophotometer. Anaerobic holo-HPPD [final concentration of 35 μM; initial concentrations of 80 μM HPPD and 70 μM Fe(II)] was prepared in a tonometer as previously described and mixed against anaerobic NTBC solutions under pseudo-first-order conditions at 5 °C (final concentrations of 0.36−4.13 mM), monitoring the increase in absorbance at 450 nm. The observed first-order rate constants were determined from a fit to a linear combination of two exponentials. The most rapid of these two rate constants exhibited an NTBC concentration dependence which was fit to eq 1.

$$k_{obs} = \frac{k_2[\text{NTBC}]}{K_1 + [\text{NTBC}]} \quad (1)$$

Formation of HPPD·Fe(II)·NTBC was also monitored with D_2O as the solvent. HPPD was concentrated at 5 °C to $\sim$2 mM ($\sim$200 μL) using a Biomax 10 kDa cutoff centrifugal filter. This solution was then diluted to 10 mL using 20 mM HEPES in D_2O (pD 7.0), concentrated to $\sim$200 μL again, and diluted to a final volume of 3 mL in 20 mM HEPES in D_2O. The holoenzyme was then prepared in a tonometer as described above [final concentration of 35 μM HPPD·Fe(II); initial concentrations of 80 μM HPPD and 70 μM Fe(II)] (99.6% D_2O). The tonometer was mounted onto the stopped-flow instrument, and the contents were mixed at 5 °C against anaerobic NTBC solutions (final concentration of 0.30−1.65 mM) dissolved in 20 mM HEPES in D_2O (pD 7.0). The increase in absorbance was monitored at 450 nm, and the data were analyzed as described above.

The wavelength dependence of the formation of the absorbance features upon NTBC association was monitored at 10 nm increments between 360 and 560 nm. A solution of anaerobic holo-HPPD [final concentration of 50 μM; initial concentrations of 110 μM HPPD and 100 μM Fe(II)] was prepared in a tonometer as described previously, and the contents were mixed under pseudo-first-order conditions against an anaerobic NTBC solution (final concentration of 2.85 mM) at 4 °C. The individual wavelength absorbance traces were combined into a single data set and spectrally deconvoluted using the singular-value decomposition kinetic analysis software, SPECFIT (Spectrum Software Associates), to determine the spectra of the species that form in the association of NTBC.

The pH dependence of the rate constants observed during association of NTBC was observed with a stopped-flow pH-jump experiment for pH values of 6.0, 7.0, and 8.0. A solution of anaerobic holo-HPPD [final concentration of 35 μM; initial concentrations of 80 μM HPPD and 70 μM Fe(II)] in 20 mM HEPES buffer (pH 7.0) was prepared in a tonometer as described above. This solution was then mixed at 4 °C under pseudo-first-order conditions against anaerobic NTBC solutions (final concentration of 0.3−4.13 mM) in 100 mM MES buffer and 100 mM HEPES buffer titrated to the target pH. The change in absorbance was monitored at 450 nm.

Reaction of HPPD·Fe(II)·NTBC with O_2. Two 4 mL solutions of 25 μM apo-HPPD, one with and one without 200 μM NTBC in 20 mM HEPES buffer (pH 7.0), were prepared anaerobically in separate tonometers at 4 °C as described above. Once the solutions were anaerobic, ferrous sulfate was added from a sidearm to achieve a final concentration of 20 μM HPPD·Fe(II) with and without NTBC, and each tonometer was mounted onto the stopped-flow instrument. A solution of oxygenated buffer was prepared by equilibrating a blend of nitrogen and oxygen to give 180 μM molecular oxygen. The oxygenated buffer was then mixed against each enzyme complex, and the oxidation of enzyme-bound Fe(II) to Fe(III) was monitored at 310 nm.

For evidence of oxidation of the HPPD·Fe(II)·NTBC complex on a longer time scale, a solution of 60 μM HPPD was made anaerobic in a 4 cm path length anaerobic cuvette by 27 alternating exchanges of vacuum and argon. Ferrous sulfate and NTBC were each added to a final concentration of 50 μM from separate sidearms to form 50 μM HPPD·Fe(II)·NTBC. The solution was then exposed to atmospheric oxygen, and spectra were recorded using a Cary 3 UV−vis spectrophotometer over a period of 2.5 days at 4 °C.

Electron Paramagnetic Resonance Spectroscopy. EPR spectroscopy was performed on a Varian E115 EPR spec-

Scheme 2

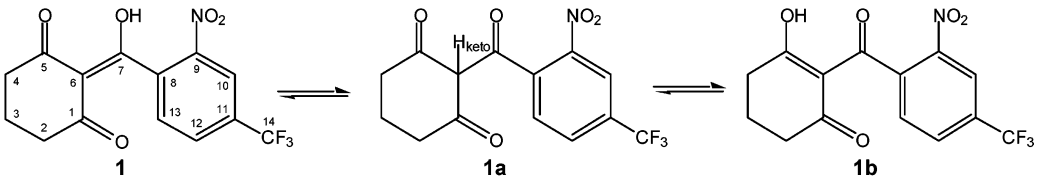

trometer with temperature control from an Air Products Helitran cryostat. Samples for EPR [HPPD·Fe(III) and HPPD·Fe(III)·NTBC] were prepared by mixing solutions of HPPD, ferric ammonium sulfate, and NTBC in 20 mM HEPES (pH 7.0). Final concentrations were as follows: 500 μM HPPD, 400 μM Fe(III), and 400 μM NTBC (for the NTBC sample).

Since HPPD·Fe(II)NO and HPPD·Fe(II)NO·NTBC samples had to be prepared under strict anaerobic conditions, all solutions were allowed to equilibrate in a Torey Pines Scientific Echotherm peltier device in an MBraun Unilab wet box for 48 h at 4 °C for removal of molecular oxygen. The solutions were then mixed in the glovebox to final concentrations of 400 μM Fe(II), 450 μM HPPD, and 500 μM NTBC (for NTBC sample) in 300 μL of 20 mM HEPES (pH 7.0). The sample was then added to a J. Young EPR tube; the tube was sealed, brought out of the glovebox, and immediately put on ice. The EPR tube was then attached to an NO Schlenk line, and the sample was nitrosylated by two cycles of vacuum and exposure to NO (1 atm).

RESULTS

Tautomeric State of NTBC in Solution. To determine the dominant tautomeric state, NMR studies were performed on a 6 mM solution of NTBC in phosphate buffer (pH 7.0). To observe protons that would exchange during enol−keto tautomerization, water was used as the solvent with just enough D_2O added to obtain a lock signal. The three most likely tautomers in aqueous solution, based on computer modeling studies by Huang *et al.* (*12*), are shown in Scheme 2. The calculated energy difference between these three tautomers is less than 16 kJ/mol, indicating that when solvent interactions are considered, any of the three could be dominant in the equilibrium.

A combination of one- and two-dimensional NMR of the ^{1}H, ^{13}C, and ^{19}F nuclei was used to identify all of the atoms that make up NTBC; chemical shifts, multiplicities, and coupling constants are given in Table 1. The only proton that was not observed in the ^{1}H spectrum is H_{keto}. Although this proton was not seen in the spectrum, it could easily have been overlapping the water peak so its absence alone does not eliminate tautomer **1a** from consideration. The use of single-bond (HSQC) and multiple-bond (HMBC) correlations between ^{13}C and either ^{1}H or ^{19}F allowed the carbon atoms to be assigned with the exception of C8 and C9, which have chemical shifts that are too similar for accurate resolution from two-dimensional spectra. Of particular importance in the identification of the tautomer are C6 and all keto−enol carbons (C1, C5, and C7). Positive identification of C7 at 191.6 ppm was from a cross-peak in the HMBC spectrum with H13 as shown in Figure 1 (inset C). Critical to identification of the correct tautomer, C1 and C5 resonated equivalently at 201.5 ppm, definitively ruling out tautomer **1b**. C6 was assigned as 115.1 ppm through a three-bond coupling to H2 in the HMBC spectrum (Figure 1, inset D). Although no single-bond ^{1}H coupling to C6 was observed in the HSQC spectrum, definitive proof of the absence of H_{keto} came from the ^{13}C DEPT spectrum (Figure 1B), which shows no peak at 115.1 ppm, indicating that C6 was not bonded to any protons. Given the above evidence, NTBC exists solely as enol **1** in aqueous solution at pH 7.0.

Table 1: NMR Data for NTBC in Aqueous Solution at pH 7.0

atom	chemical shift (ppm)	multiplicity	sign of DEPT	*J* (Hz)
C1, C5	201.5	1		
C2, C4	38.1	1	−	
C3	19.6	1	−	
C6	115.1	1		
C7	191.6	1		
C8, C9	144.9, 145.1	1		
C10	121.9	1	+	
C11	130.1	4		40
C12	131.8	1	+	
C13	127.7	1	+	
C14	123.5	4		270
H2, H4	2.6	3		6
H3	2.1	5		6
H10	8.7	1		
H12	8.2	2		8
H13	7.6	2		8

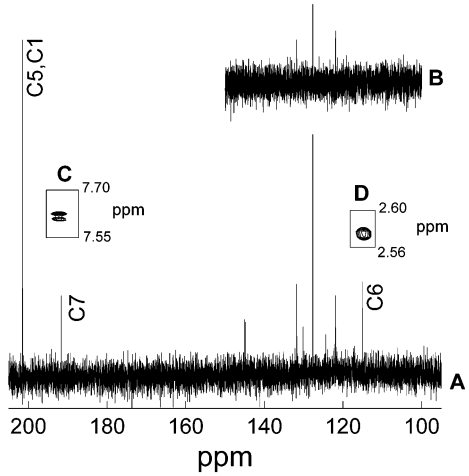

FIGURE 1: ^{13}C NMR spectra of NTBC. NMR spectra were recorded on a 500 MHz Bruker NMR spectrometer. NTBC was dissolved in 20 mM phosphate buffer (pH 7.0) to a final concentration of 6 mM: (A) ^{13}C NMR spectrum, (B) ^{13}C DEPT spectrum, (C) ^{1}H-{^{13}C}HMBC cross-peak for C7, and (D) ^{1}H{^{13}C}HMBC cross-peak for C6.

Evidence of Steady-State Inhibition. Although NTBC has been shown to inhibit HPPD from both mammals (*22*, *28*, *29*) and plants (*4*), inhibition of a bacterial HPPD has not been previously demonstrated. Inhibition was shown during a steady-state assay while the dissolved oxygen concentration was being monitored. Fifteen seconds after initiation with HPP, NTBC was added, and within 10 s, oxygen consump-

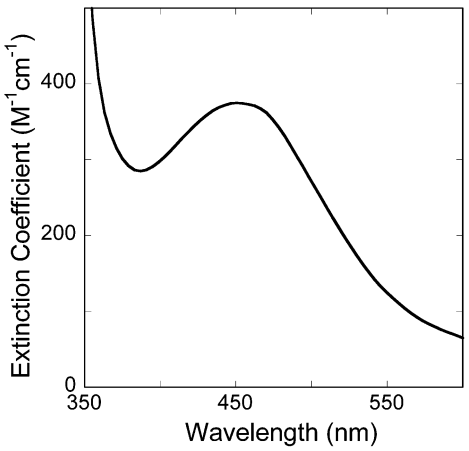

FIGURE 2: Difference spectrum of NTBC bound to HPPD·Fe(II). The spectrum was of 200 μM HPPD·Fe(II)·NTBC in 20 mM HEPES (pH 7.0). The contributions of HPPD·Fe(II) and free NTBC were subtracted.

tion had returned to the background rate due to free iron(II) undergoing Fenton chemistry in the presence of DTT. HPPD from *S. avermitilis* is thus fully inhibited by NTBC.

Binding of NTBC to HPPD. When HPP or another monoanionic α-keto acid is bound to HPPD·Fe(II), a charge-transfer band at ~500 nm is observed (*26*). Although NTBC is not an α-keto acid, when it was added anaerobically to the holoenzyme, a similar absorbance band at 450 nm was formed (Figure 2). The observation of this feature provided evidence that NTBC binds to the metal center of the active ferrous form of the enzyme. In contrast, no binding feature was observed between 300 and 800 nm when NTBC is mixed with HPPD·Fe(III). Also, no perturbation was observed in the EPR spectrum of HPPD·Fe(III) at 15 K when NTBC was added in a 1:1 ratio. Since there is no change in the EPR spectrum, if NTBC does associate with the ferric form of HPPD, it does so weakly (K_d > 1 mM) or is not liganded to the active site metal ion.

The kinetics of formation of the HPPD·Fe(II)·NTBC absorbance feature were monitored at 450 nm using a stopped-flow spectrophotometer. The absorbance traces (Figure 3) were fit to the sum of two exponentials. The magnitude of the faster phase (Figure 3 inset) had a hyperbolic dependence on NTBC concentration. The slower phase was approximately 25% of the total amplitude change at saturating levels of NTBC, and its rate constant was independent of the NTBC concentration. These data are consistent with a pre-equilibrium (K_1 = 1.25 ± 0.08 mM) preceding two irreversible steps (k_2 = 8.2 ± 0.2 s^{-1}; k_3 = 0.76 ± 0.02 s^{-1}) that form spectrophotometrically distinct species. The formation of the HPPD·Fe(II)·NTBC complex was also monitored with D_2O as the solvent. Because of the decreased solubility of NTBC in D_2O (~3 mM), a more narrow range of NTBC concentrations was used. Within experimental error, K_1 was unchanged, and fixing K_1 to equal the value observed in H_2O (1.25 mM) does not decrease the quality of the fit as measured by the *R* value. The limiting rate shows an isotope effect of 1.3 (k_2 = 6.5 ± 0.1 s^{-1}), while an isotope effect of 3 is observed on k_3 (0.24 ± 0.05 s^{-1}; Figure 3 inset). Proton transfers were therefore involved in the processes of the formation of the inhibitor complex.

Deconvolution of the wavelength dependence data at a single concentration of NTBC revealed the spectra of the

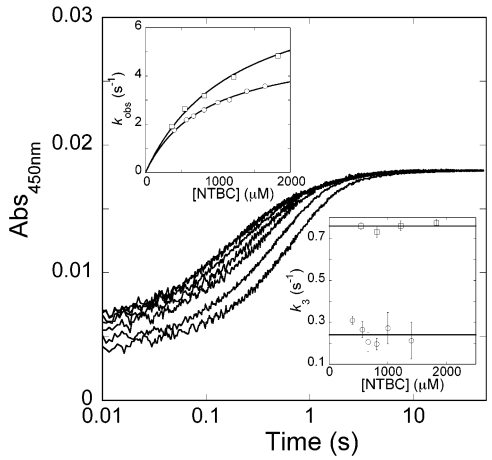

FIGURE 3: Kinetics of binding of NTBC to HPPD·Fe(II). HPPD·Fe(II) (final concentration of 35 μM) was mixed vs various NTBC concentrations (final concentration of 362 μM to 4.13 mM) and monitored at 450 nm and 5 °C. The absorbance traces shown are for 362, 543, 814, 1220, 1830, 2750, and 4130 μM NTBC. The traces were fit to two exponentials and the observed rate constants replotted vs NTBC concentration with both H_2O (□) and D_2O (○) as the solvent (insets).

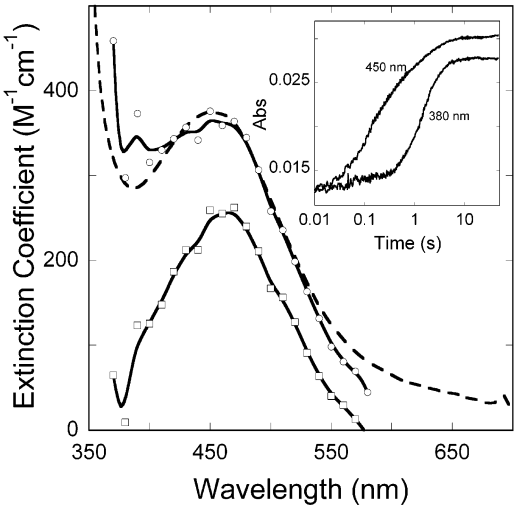

FIGURE 4: Difference spectra of the charge-transfer species observed in binding to the ferrous holoenzyme under anaerobic conditions. HPPD·Fe(II) (final concentration of 50 μM) was mixed with NTBC (final concentration of 2.85 mM) and the reaction monitored at 10 nm increments between 360 and 560 nm at 4 °C. These data were fit globally to two phases to derive the spectra of the binding intermediate (□) and the final HPPD·FeII·NTBC complex (○). For comparison, the deconvoluted spectra are shown overlaid with the independently determined final HPPD·FeII·NTBC complex difference spectrum (− − −). The inset depicts representative absorbance changes at 380 and 450 nm.

two colored species observed during the association of NTBC with the ferrous holoenzyme (Figure 4). The first of these has a broad visible absorbance whose maximum extinction coefficient was 250 M^{-1} cm^{-1} at 460 nm. This intermediate binding complex then decayed to the final complex whose visible maximum was 450 nm and which had increased absorbency (370 M^{-1} cm^{-1}). The primary spectrophotometric difference between the two species was the 300 M^{-1} cm^{-1} absorbance increase at 380 nm observed in the final complex. This difference is directly evident when individual absorbance changes at each of these wavelengths are compared (Figure 4 inset).

Scheme 3

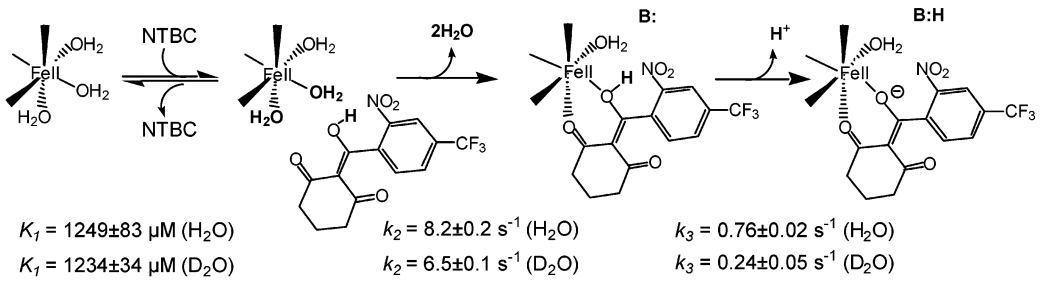

The pH dependence of the equilibrium constant K_1 and rate constants k_2 and k_3 for NTBC association were measured for pH values of 6.0, 7.0, and 8.0. The purpose of these experiments was to assess if an active site base involved in proton transfers during NTBC association could be titrated and also to ensure that observed kinetic isotope effects were not a consequence of differences in the fractional protonation state of such a base in D_2O versus H_2O solvent. For each pH value, the observed kinetic traces could be fit to two phases, indicating that no additional kinetic steps were evident. Moreover, K_1, k_2, and k_3 exhibited no dependence on pH in this range. Within the limits of error, for pH values of 6.0 and 8.0, K_1, k_2, and k_3 were unchanged from those observed in previous experiments. This is evidence that any active site base directly involved in NTBC association has a pK_a value of less than 5.5 and/or is insensitive to solvent proton concentrations in the HPPD·Fe(II)·NTBC complex. Furthermore, kinetic isotope effects observed in D_2O are not a result of a fractional population of such a base in this solvent.

A proposed mechanism consistent with these data is given in Scheme 3. In this model, NTBC binds initially reversibly proximal to the active site metal ion defined by the dissociation constant K_1 and k_2 is the subsequent bidentate association with the Fe(II) atom producing an initial charge-transfer absorbance. In k_3, the Lewis-acidic metal ion assists in the irreversible deprotonation of the enol to form the enolate complex, producing a second and final charge-transfer band with a slightly increased intensity.

Reaction of Dioxygen and Nitric Oxide with HPPD·Fe(II)·NTBC. The holoenzyme, both free and in complex with HPP, reacts with molecular oxygen (*26*). Oxidation can be monitored at 310 nm as the Fe(III) form of HPPD has significant absorbance in this region of the spectrum. Surprisingly, HPPD·Fe(II) in complex with NTBC exhibited no evidence of oxidation. In contrast to the holoenzyme, there was no increase in absorbance at 310 nm upon mixing of HPPD·Fe(II)·NTBC with molecular oxygen (Figure 5).

To observe the long-term aerobic stability and to measure the dissociation rate constant for HPPD·Fe(II)·NTBC, the complex was made anaerobically and exposed to molecular oxygen, and spectra were recorded over a period of 2.5 days. Since the holoenzyme oxidizes at a rate of 0.015 s^{-1} (390 μM oxygen), if NTBC were released from the enzyme at an appreciable rate, oxidation of the holoenzyme should be observed. Simulation of the proposed kinetic model incorporating the known oxidation rate of the free enzyme confirmed that oxidation of the enzyme would be concomitant with NTBC release. The absorbance feature showed no decrease over 2 days (Figure 5 inset), meaning that the complex did not oxidize [the Fe(III) form has no absorbance at 450 nm]. The sensitivity of this method with regard to the instrument that was used would have permitted the observation of dissociation rates of as low as 2×10^{-7} s^{-1}. The lack of reactivity showed that the HPPD·Fe(II)·NTBC complex was extremely stable in air and the off rate of NTBC could not be measured under the conditions of the experiment.

Nitric oxide is a useful surrogate for molecular oxygen with ferrous iron-dependent enzymes because it allows the iron center to be readily examined by EPR spectroscopy and does not continue on a reactive pathway yet is geometrically similar to oxygen in coordination (*30*, *31*). The holoenzyme reacted readily with nitric oxide to form an $S = {}^3/_2$ species with an axial EPR $g_\perp = 3.95$ signal; the $g_\parallel \sim 2$ signal is overlapped by free NO (Figure 6). When the NTBC-bound holoenzyme is exposed to nitric oxide, only a small fraction (~2%) of the enzyme reacted with NO over the course of 1 h, which was consistent with the observed lack of oxygen reactivity.

DISCUSSION

Knowing the tautomeric configuration of NTBC under biologically relevant conditions may be important in understanding its inhibitory mechanism toward HPPD. It has been

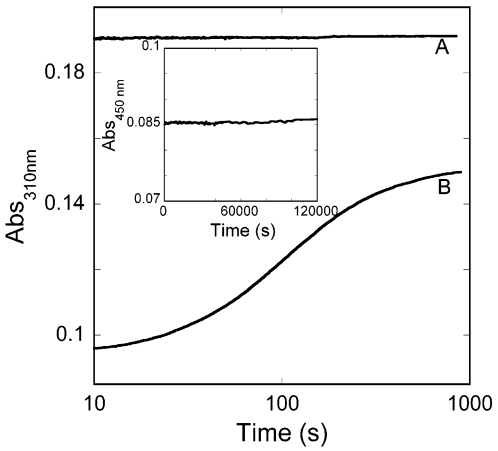

FIGURE 5: Oxidative stability of the HPPD·Fe(II)·NTBC complex relative to the free holoenzyme. The HPPD·Fe(II)·NTBC complex at 4 °C (A) or the HPPD·Fe(II) complex (B) (final concentration of 20 μM) was mixed vs oxygen (final concentration of 180 μM), and the absorbance was monitored at 310 nm. Note that the elevated absorbance of trace A relative to trace B is due to the underlying absorbance contribution of free and bound NTBC. In the inset, the HPPD·Fe(II)·NTBC complex was prepared anaerobically and then allowed to react with atmospheric oxygen over a period of 2 days. The absorbance at 450 nm was plotted vs time.

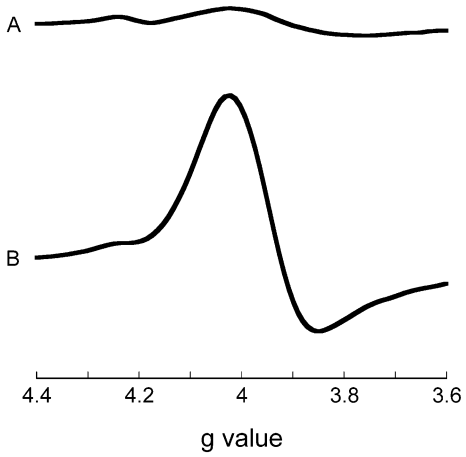

FIGURE 6: EPR spectra of HPPD·Fe(II)·NTBC (A) and HPPD·Fe(II) (B) in the presence of nitric oxide. Spectra were recorded for 400 μM samples at 21 K on a Varian EPR spectrometer. Instrumental conditions: microwave power of 1 mW, microwave frequency of 9.27 GHz, modulation frequency of 100 kHz, modulation amplitude of 8 G, and receiver gain of 5000.

proposed that direct correlations exist between the tautomeric population in solution and the observed inhibitory activity. Theoretical calculations performed by Huang *et al*. on similar triketones suggested that the two dominant tautomeric forms in solution would be the exocyclic and endocyclic enols (**1** and **1b**, respectively) (*12*). Subsequent structure−activity relationships elucidated by Huang *et al*. were, however, based solely on the endocyclic form. X-ray crystallographic analysis by Wu *et al*. of a triketone that is missing the trifluoromethyl group of NTBC showed that the solid-state configuration is the endocyclic enol, although the bond lengths show some exocyclic enol character (*25*). Previous NMR studies performed in chloroform also showed the three enol−keto carbon atoms consistent with the endocyclic enol (*25*). The NMR studies presented herein were performed in aqueous solution at pH 7.0. These studies showed that there are two symmetrically inequivalent enol−keto carbon atoms whose identity indicated that the exocyclic enol is dominant ($\geq$95%). Though a number of articles have quoted the endocyclic enol as the dominant state, the subtle structural difference between this and the exocyclic tautomer would not have necessarily rendered invalid the conclusions that were drawn.

With the exception of the studies on carrot HPPD (*8*), all literature K_i and IC_{50} values for HPPD interacting with this class of inhibitors have been determined with the partially purified or crude enzyme; this potentially leads to fundamental problems with interpretation of the measurements. For example, one-step binding and release are assumed because more complicated kinetic mechanisms are not generally observable in such mixtures. In particular, spectroscopic investigations of binding and release processes are complicated by the presence of numerous signals from various components of the mixture such as constantly changing ratios of Fe(II) and Fe(III) forms of the enzyme (*26*). Moreover, in the absence of experiments that accurately define the dissociation rate constants, IC_{50} values either genuinely describe the equilibrium of the free enzyme and inhibitor with the enzyme−inhibitor complex or are simply a measurement of one-half of the enzyme concentration mediated by the incubation time prior to measurement.

The mode of action of NTBC inhibition is not well understood; conjecture has even existed about whether NTBC binds predominantly to the ferric or ferrous forms of HPPD. Prisbylla *et al*. (*6*) initially proposed that the triketone inhibitor is structurally similar to the substrate HPP and hence will bind to the active ferrous form of the enzyme. This idea was supported by the fact that the diketone moiety seems to be the minimum requirement for effective inhibition (*2*, *10*, *13*). Using a radiolabeled inhibitor, Garcia *et al*. (*8*) showed that a diketone inhibitor bound to the ferrous form of HPPD and not to the ferric form. In contrast, on the basis of the correlation between the strength of binding of triketone inhibitors to Fe(III) in solution and their inhibitory strength, it was proposed by Wu *et al*. (*25*) that the ferric form of HPPD is the relevant oxidation state for inhibition. We have definitively shown that NTBC interacts with ferrous HPPD; a metal-centered absorbance at 450 nm is formed when NTBC is added to HPPD·Fe(II). Additionally, no spectroscopic changes in the UV−vis or EPR spectra were seen upon mixing of NTBC and ferric HPPD, indicating that binding to the ferric form, if it occurs, is not the dominant mode of inhibition. These observations are in agreement with the majority of the previous proposals that support inhibition occurring on the active ferrous form of HPPD.

The number of steps in the binding mechanism of NTBC has not been previously established. Ellis *et al*. (*29*) have observed the slow onset of inhibition, suggesting that NTBC associates with HPPD slowly. The observation of a weak charge-transfer band for the HPPD·Fe(II)·NTBC complex afforded an opportunity to define the binding mechanism. The hyperbolic dependence of the rate of development of the initial charge-transfer band on NTBC concentration was consistent with a pre-equilibrium and a subsequent limiting association that produces the initial absorbance band (Scheme 3). The kinetic isotope effect of 1.3 on this step (k_2) is possibly a secondary effect associated with the displacement of water from the active site metal ion. A kinetic isotope effect of 3 on the subsequent processes (k_3) suggests that proton movement is involved in this process also. Since the apparently primary isotope effect coincided with the formation of the second charge-transfer absorbance, we have proposed the formation of an irreversible enolate that is bound bidentate to the active site Fe(II) atom. The irreversibility of this step is proposed because the HPPD·Fe(II)·NTBC complex had no oxygen reactivity even over an extended period of time. The lack of oxygen reactivity is consistent with a proposal based on computer-generated structural alignment by Hanauske-Abel *et al*. (*32*) that the nitro group of NTBC is positioned to block access for molecular oxygen to the iron atom. Given that the oxygen reactivity of the HPPD holoenzyme is known (*26*), it is possible to definitively state that oxidation of the HPPD·Fe(II)·NTBC complex to form the colorless ferric form would be concomitant with NTBC release; therefore, the lack of oxidation over a period of 2.5 days signifies a lack of NTBC dissociation.

There are many factors that determine reversibility. Ellis *et al*. (*33*) observed the recovery of 90% of HPPD activity from crude rat cytosol over the course of 10 h, implying slow dissociation. The irreversibility observed for HPPD from *S. avermitilis* may be species specific; however, the parameters concerning association and dissociation have now

been clearly established for this species. It is a requirement that the extent or rate of dissociation be known before an observed IC_{50} or K_i value is an accurate representation of the binding constant or structure−activity relationships are meaningful in the development of new inhibitors.

ACKNOWLEDGMENT

We thank F. Holger Fosterling for his assistance with the NMR studies. We are grateful to Dr. Arsenio Pacheco of the Department of Chemistry and Biochemistry at the University of Wisconsin−Milwaukee for the use of his NO Schlenk line and glovebox. We thank Swedish Orphan AB for supplying the NTBC used in this study. We also express our gratitude to Richard and Joan Miller for the generous donation of the Helium dewar, transfer line, and cold finger used in the EPR experiments.

REFERENCES

1. Hellyer, R. (1968) *Aust. J. Chem. 21*, 2825−2828.
2. Romagni, J. G., Meazza, G., Nanayakkara, N. P., and Dayan, F. E. (2000) *FEBS Lett. 480*, 301−305.
3. Gray, R. A., Russay, R. J., and Tseng, C. K. (1980) U.S. Patent 4,202,840.
4. Schulz, A., Ort, O., Beyer, P., and Kleinig, H. (1993) *FEBS Lett. 318*, 162−166.
5. Secor, J. (1994) *Plant Physiol. 106*, 1429−1433.
6. Prisbylla, M. P., Onisko, B. C., Shribbs, J. M., Adams, D. O., Liu, Y., Ellis, M. K., Hawkes, T. R., and Mutter, L. C. (1993) *Brighton Crop Prot. Conf.-Weeds*, 731−738.
7. Goodwin, T. W., and Mercer, E. I. (1983) *Introduction to Plant Biochemistry*, 2nd ed., Pergamon Press, Sydney.
8. Garcia, I., Job, D., and Matringe, M. (2000) *Biochemistry 39*, 7501−7507.
9. Lin, S. W., Lin, Y. L., Lin, T. C., and Yang, D. Y. (2000) *Bioorg. Med. Chem. Lett. 10*, 1297−1298.
10. Lin, Y. L., Wu, C. S., Lin, S. W., and Yang, D. Y. (2000) *Bioorg. Med. Chem. Lett. 10*, 843−845.
11. Huang, M., Yang, D. Y., Shang, Z., Zou, J., and Yu, Q. (2002) *Bioorg. Med. Chem. Lett. 12*, 2271−2275.
12. Huang, M. L., Zou, J. W., Yang, D. Y., Shang, Z. C., and Yu, Q. S. (2002) *J. Mol. Struct. 589*−*590*, 321−328.
13. Pallett, K. E., Cramp, S. M., Little, J. P., Veerasekaran, P., Crudace, A. J., and Slater, A. E. (2001) *Pest Manage. Sci. 57*, 133−142.
14. Mitchell, G., Bartlett, D. W., Fraser, T. E., Hawkes, T. R., Holt, D. C., Townson, J. K., and Wichert, R. A. (2001) *Pest Manage. Sci. 57*, 120−128.
15. Sutton, P., Richards, C., Buren, L., and Glasgow, L. (2002) *Pest Manage. Sci. 58*, 981−984.
16. Huhn, R., Stoermer, H., Klingele, B., Bausch, E., Fois, A., Farnetani, M., Di Rocco, M., Boue, J., Kirk, J. M., Coleman, R., and Scherer, G. (1998) *Hum. Genet. 102*, 305−313.
17. Phornphutkul, C., Introne, W. J., Perry, M. B., Bernardini, I., Murphey, M. D., Fitzpatrick, D. L., Anderson, P. D., Huizing, M., Anikster, Y., Gerber, L. H., and Gahl, W. A. (2002) *N. Engl. J. Med. 347*, 2111−2121.
18. Russo, P., and O'Regan, S. (1990) *Am. J. Hum. Genet. 47*, 317−324.
19. Russo, P. A., Mitchell, G. A., and Tanguay, R. M. (2001) *Pediatr. Dev. Pathol. 4*, 212−221.
20. Lindblad, B., Lindstedt, S., and Steen, G. (1977) *Proc. Natl. Acad. Sci. U.S.A. 74*, 4641−4645.
21. Michaely, W. J., and Kratz, G. W. (1988) U.S. Patent 4,780,127.
22. Lindstedt, S., Holme, E., Lock, E. A., Hjalmarson, O., and Strandvik, B. (1992) *Lancet 340*, 813−817.
23. Ahmad, S., Teckman, J. H., and Lueder, G. T. (2002) *Am. J. Ophthalmol. 134*, 266−268.
24. Holme, E., and Lindstedt, S. (1998) *J. Inherited Metab. Dis. 21*, 507−517.
25. Wu, C. S., Huang, J. L., Sun, Y. S., and Yang, D. Y. (2002) *J. Med. Chem. 45*, 2222−2228.
26. Johnson-Winters, K., Purpero, V. M., Kavana, M., Nelson, T., and Moran, G. R. (2003) *Biochemistry 42*, 2072−2080.
27. Sklenar, V., Piotto, M., Leppik, R., and Saudek, V. (1993) *J. Magn. Reson., Ser. A 102*, 241−245.
28. Hall, M. G., Wilks, M. F., Provan, W. M., Eksborg, S., and Lumholtz, B. (2001) *Br. J. Clin. Pharmacol. 52*, 169−177.
29. Ellis, M. K., Whitfield, A. C., Gowans, L. A., Auton, T. R., Provan, W. M., Lock, E. A., and Smith, L. L. (1995) *Toxicol. Appl. Pharmacol. 133*, 12−19.
30. Hegg, E. L., Whiting, A. K., Saari, R. E., McCracken, J., Hausinger, R. P., and Que, L., Jr. (1999) *Biochemistry 38*, 16714−16726.
31. Brown, C. A., Pavlosky, M. A., Westre, T. E., Zhang, Y., Hedman, B., Hodgson, K. O., and Solomon, E. I. (1995) *J. Am. Chem. Soc. 117*, 715−732.
32. Hanauske-Abel, H. M., Popowicz, A., Remotti, H., Newfield, R. S., and Levy, J. (2002) *J. Pediatr. Gastroenterol. Nutr. 35*, 73−78.
33. Ellis, M. K., Whitfield, A. C., Gowans, L. A., Auton, T. R., Provan, W. M., Lock, E. A., Lee, D. L., and Smith, L. L. (1996) *Chem. Res. Toxicol. 9*, 24−27.

BI034658B